



Sign up for PNAS Online eTocs

Get notified by email when
new content goes on-line

[Info for Authors](#) | [Editorial Board](#) | [About](#) | [Subscribe](#) | [Advertise](#) | [Contact](#) | [Site Map](#)

PNAS

Proceedings of the National Academy of Sciences of the United States of America

Current Issue

Archives

Online Submission

GO

[advanced search >>](#)

Institution: CB# 3938 DAVIS LIBRARY | [Sign In via User Name/Password](#)

Serohijos *et al.* 10.1073/pnas.0800254105.

Supporting Information

Files in this Data Supplement:

[SI Text](#)

[SI Figure 5](#)

[SI Figure 6](#)

[SI Figure 7](#)

[SI Figure 8](#)

[SI Figure 9](#)

[SI Figure 10](#)

[SI Figure 11](#)

This Article

› [Abstract](#)

› [Full Text](#)

Services

› [Email this article to a colleague](#)

› [Alert me to new issues of the journal](#)

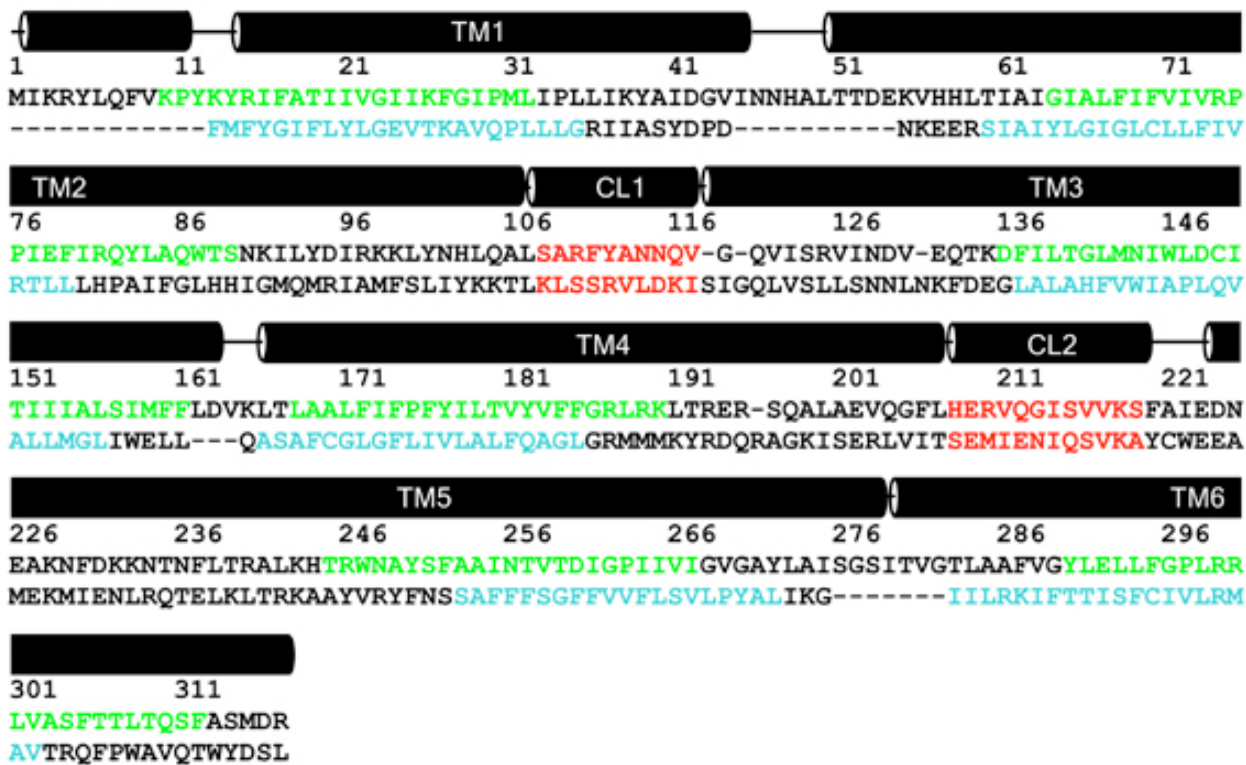
› [Request Copyright Permission](#)

Citing Articles

› [Citing Articles via CrossRef](#)

> Sav1866 MSD

> CFTR MSD1



> Sav1866 MSD

> CFTR MSD2

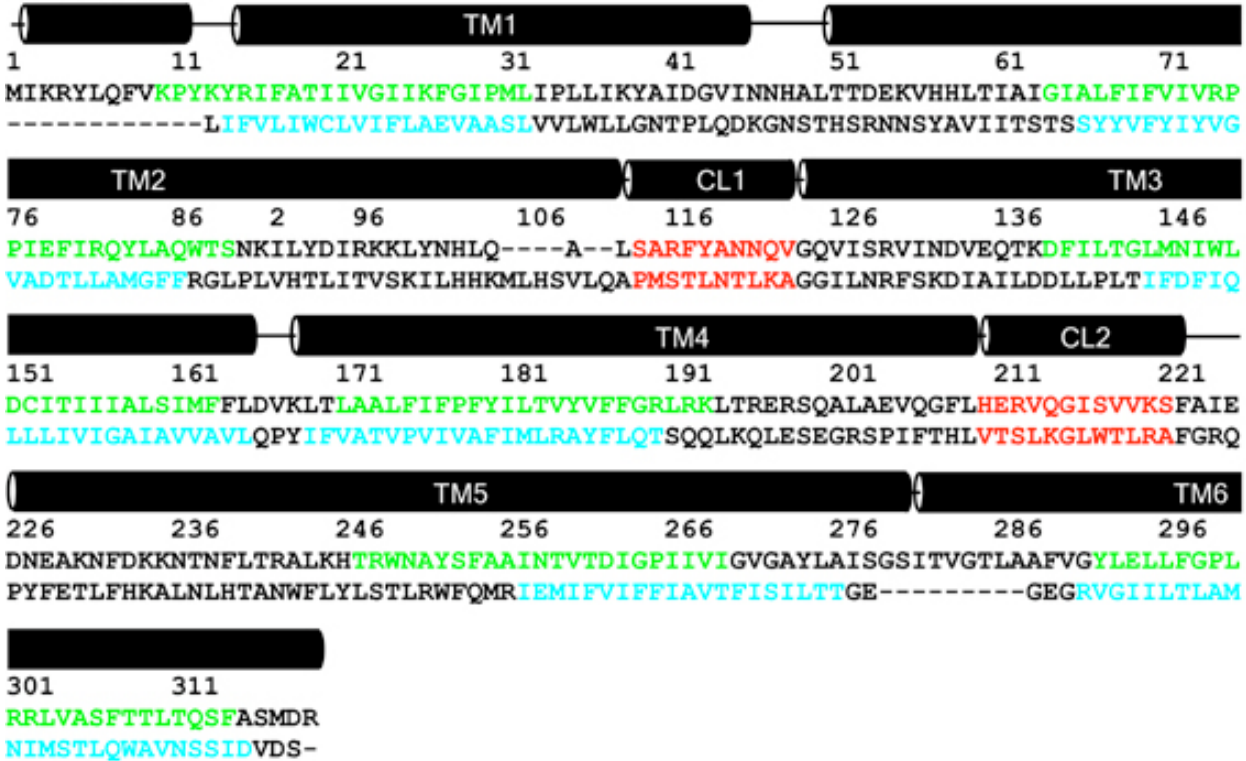


Fig. 5. Sequence alignment of the membrane-spanning domains of human CFTR (GenBank accession no. P13569) (1) and the Sav1866 exporter (3). Predicted membrane-embedded regions of Sav1866 are colored green, and those of CFTR are blue. Coupling helices are red.

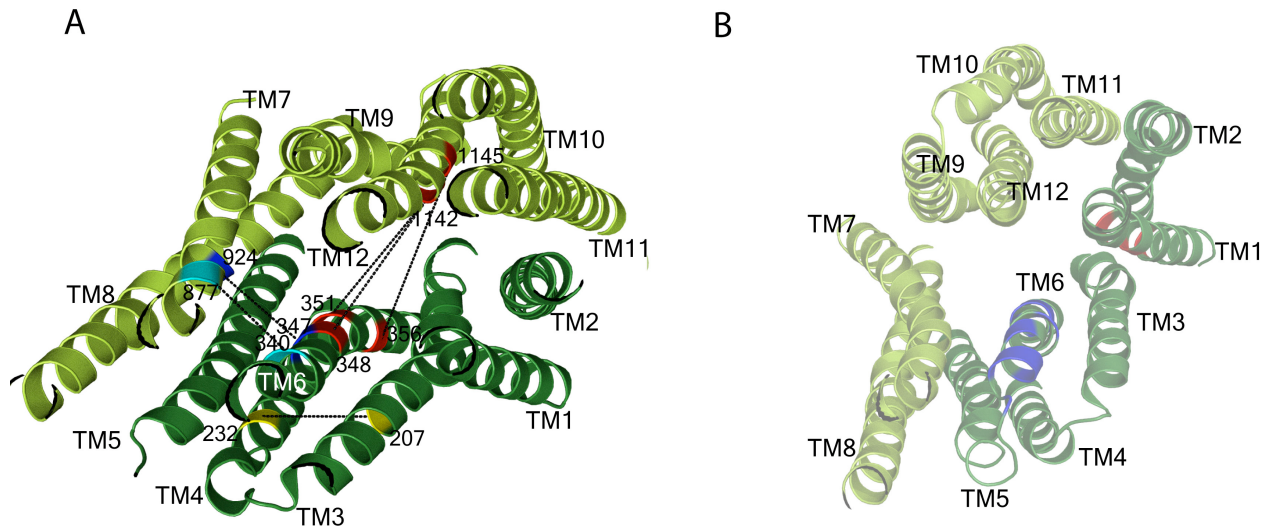


Fig. 6. Experimental constraints satisfied in the membrane-spanning domains of the homology model. (A) Cross-links can be formed between M348-T1142, T351-T1142, and W356-T1145 (red), which are pairs of residues found between TM6 and TM12 (9). R347 (TM6) forms a salt bridge with D924 (TM8) (blue) (11). A H-bond can be formed between Q207 (TM3) and V232 (TM4) (yellow) (12). A recent constraint from cross-linking of I340C-S877C (cyan) is also satisfied (10). (B) Residues G91, K95, and Q98 (colored red) in TM1 are water-accessible, suggesting that they face the channel pore (13). I331, L333, R334, K335, F337, S341, R347, T351, R352, and Q353 (colored blue), which are all found in TM6, are also water-accessible (14).

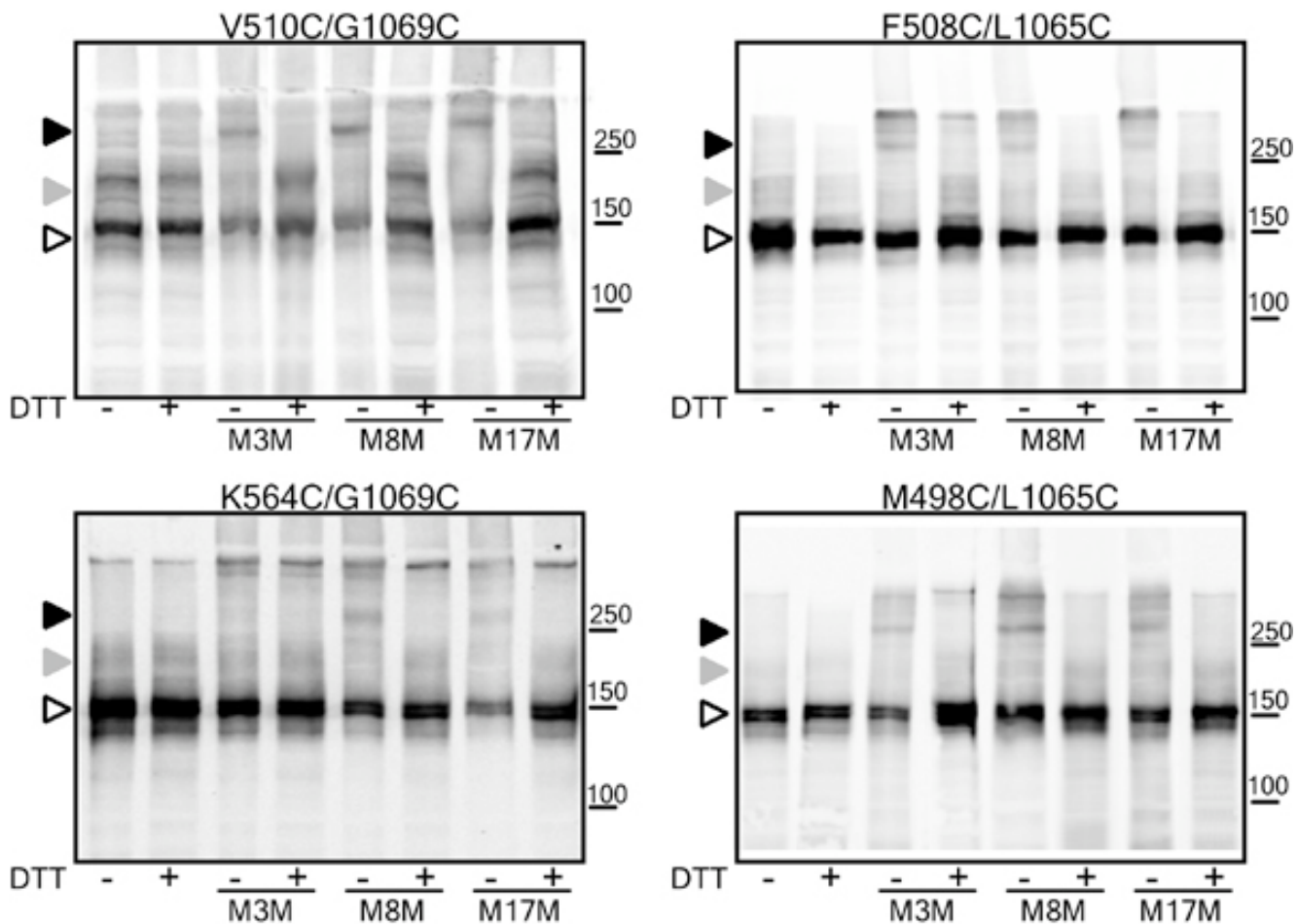


Fig. 7. Additional cross-linking at the CL4 and NBD1 interface. Cross-linking was performed on intact cells as described in the *SI Methods*. Open arrowheads, immature core-glycosylated CFTR (band B); gray arrowheads, mature complex-glycosylated CFTR (band C); black arrowheads, cross-linked mature protein.

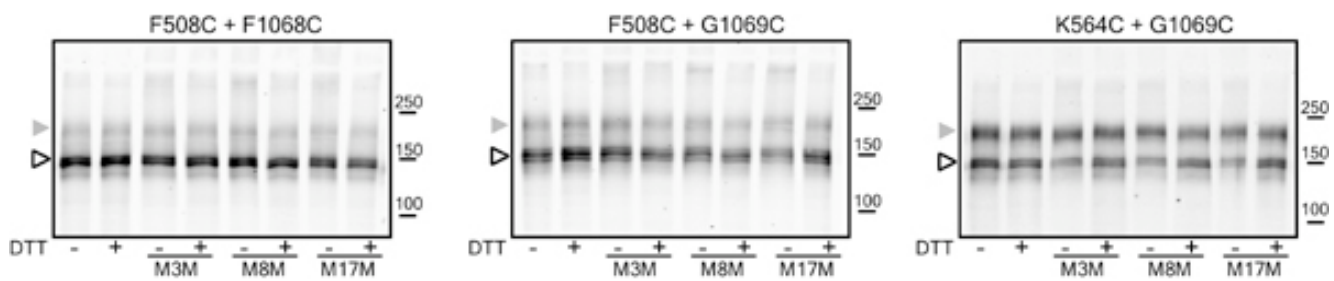


Fig. 8. Cross-linking controls. Cross-linking was performed on intact HEK293 cells coexpressing constructs with single cysteines. Cells were exposed to MTS cross-linkers, and no cross-linking was detected. Open arrowheads, band B; gray arrowheads, band C.

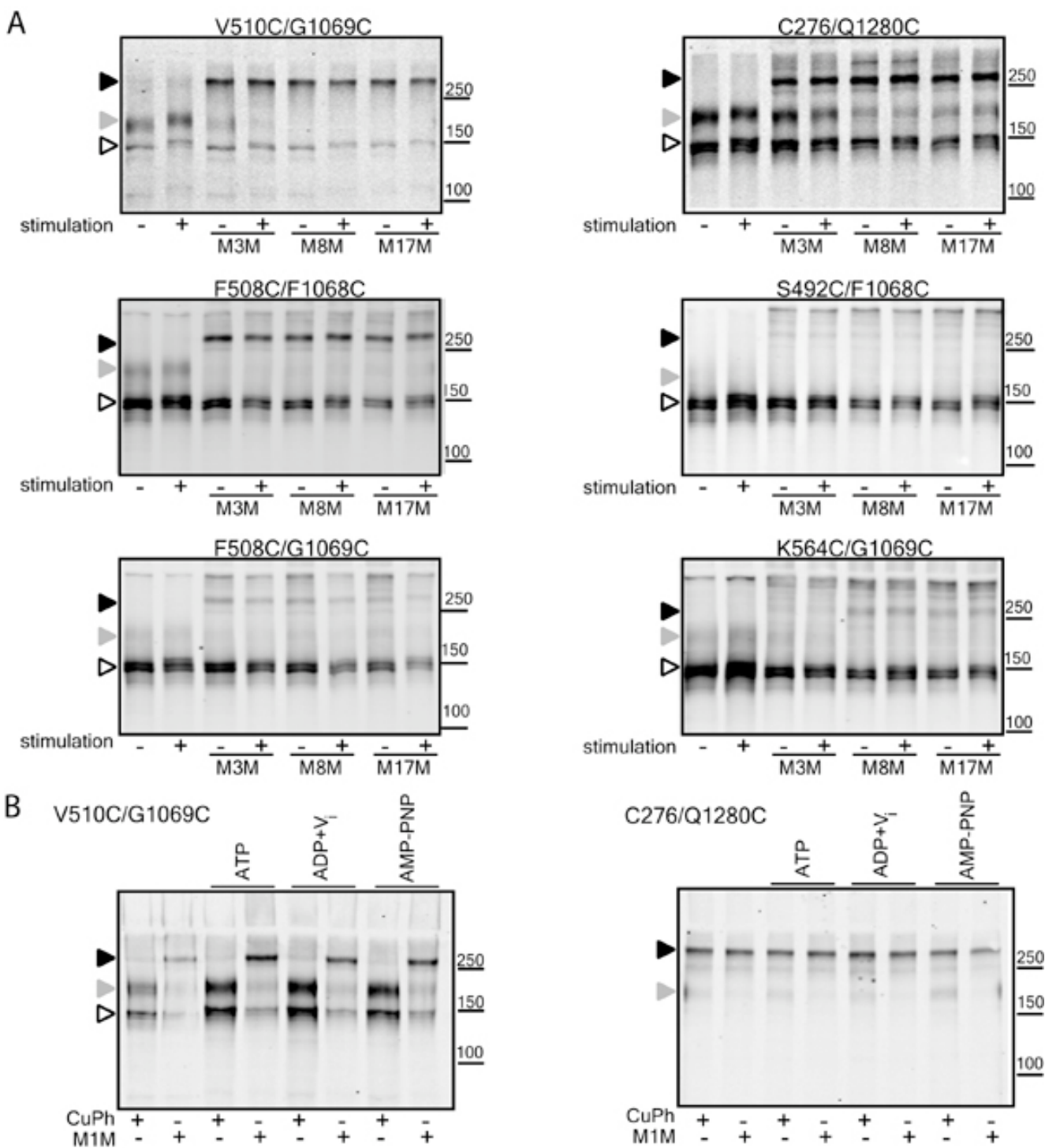


Fig. 9. Lack of effect of phosphorylation and nucleotides on cross-linking. (A) Phosphorylation by PKA does not alter cross-linking. Cells were harvested and treated with stimulation mixture (10 μ M forskolin, 100 μ M DiBu-cAMP, and 1 mM IBMX) for 5 min. Cross-linking was performed in the presence of the stimulation mixture. (B) Nucleotides influencing CFTR function do not affect cross-linking. Membranes isolated from cells expressing double cysteine constructs were pretreated with purified PKA catalytic

subunit and ATP. After washing, the membranes were incubated with 5 mM ATP, ADP plus vanadate (V_i), or AMP-PNP for 5 min, and the cross-linking was promoted with copper phenanthroline or M1M for an additional 15 min. CFTR was detected by anti-CFTR mAb596. Open arrowheads, band B; gray arrowheads, band C; black arrowheads, cross-linked mature protein.

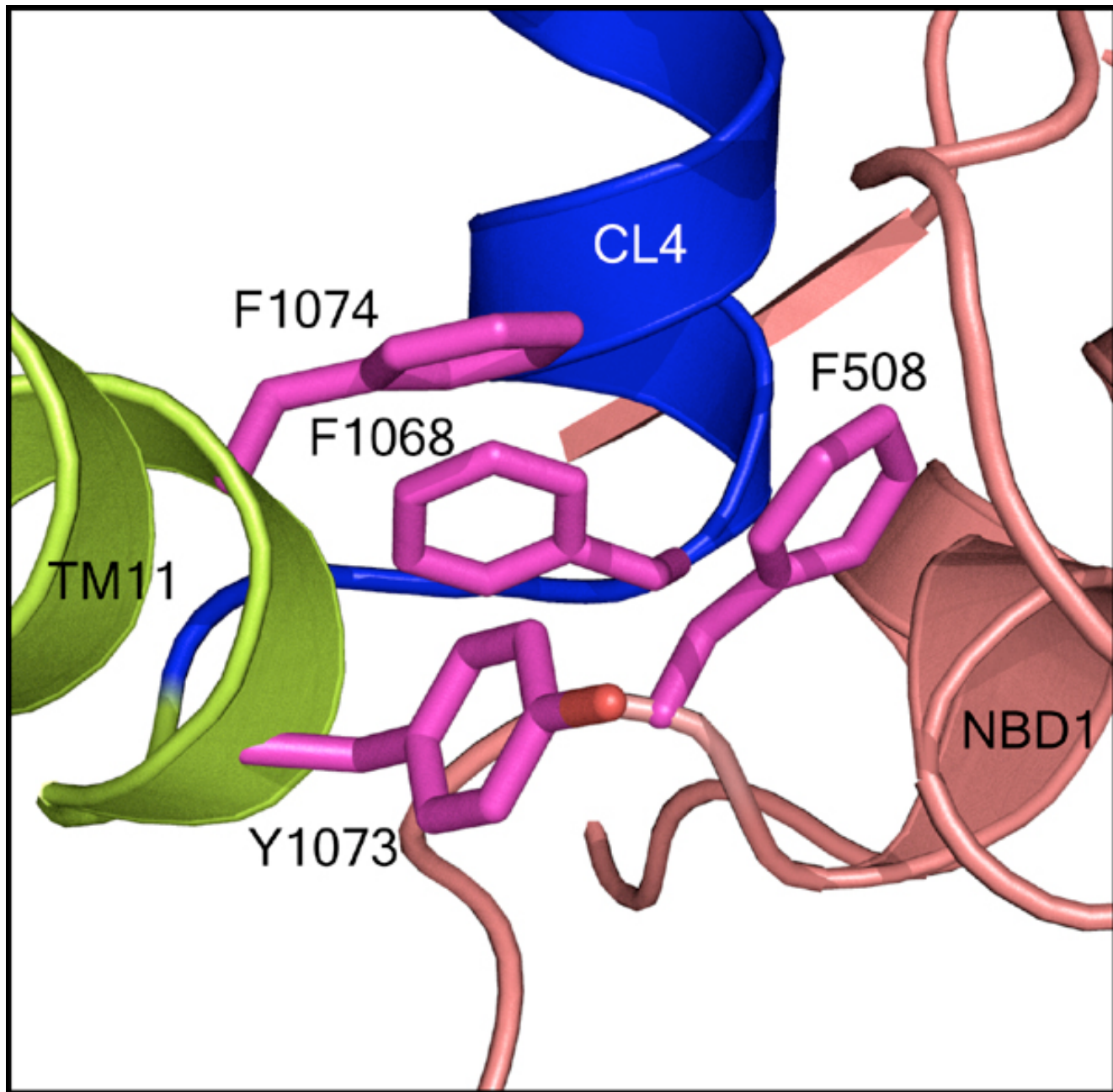


Fig. 10. Cluster of aromatic residues including Phe-508 at the NBD1/CL4 interface.

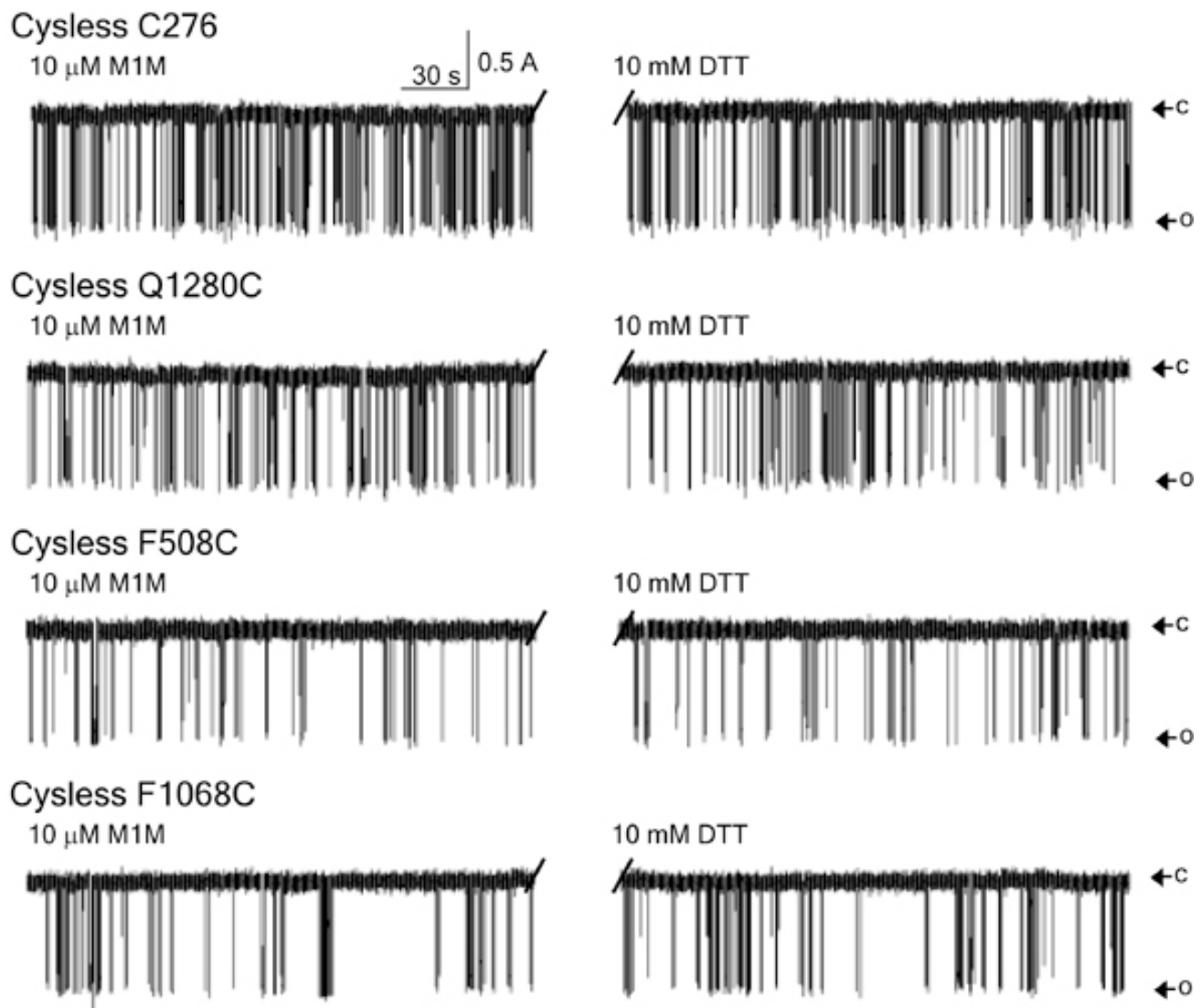


Fig. 11. Lack of effect of MTS cross-linker on single-channel activity of constructs containing single cysteines that contribute to cross-linkable pairs.

SI Text

Structural Modeling of Complete Cystic Fibrosis Transmembrane Conductance Regulator (CFTR). CFTR (GenBank accession no. P13569) (1) consists of several domains: nucleotide-binding domains NBD1 and NBD2, membrane-spanning domains MSD1 and MSD2, and a regulatory R domain. There are existing crystal structures of NBD1 [Protein Data Bank (PDB) ID code 2BBO] but none for the other domains. The missing regulatory loop in NBD1 was inserted from a loop database search in SYBYL (Tripos, Inc.). The NBD1-NBD2 dimer was constructed by superimposing the NBD1 crystal structure and the homology model of NBD2 (2) on the Sav1866 (PDB ID code 2HYD) structure (3). All of the inter-NBD cross-links observed by Mense *et al.* (4) are accommodated by the model.

Because both CFTR and Sav1866 contain 12 transmembrane helices that are of similar length, we opted to model the CFTR membrane-spanning domains from that of Sav1866. The alignment of Sav1866 and CFTR was dictated by the position of their corresponding membrane-embedded regions and the conserved coupling helices in the intracellular loops (SI Fig. 5). The membrane-embedded regions of the Sav1866 helices were identified from the PDB_TM database (5), whereas the approximate locations of CFTR TM helices were defined by using the results from earlier glycosylation site insertions (6) and the HMMTOP transmembrane prediction server (www.enzim.hu/hmmtop) (7). Using the CFTR-Sav1866 alignment, the atomic model of CFTR MSDs was constructed in the Homology suite of INSIGHTII (Accelrys, Inc.). To eliminate clashes and refine the model, the side-chain rotamer states were optimized, and minor backbone fluctuations were introduced by using Medusa (8).

The structural model is consistent with available experimental data on the orientation and packing of transmembrane helices. Pairs of residues such as M348C/T1142C, T351C/T1142C, and W356C/W1145C, which come from transmembrane helices TM6 and TM12, could be cross-linked by molecules of different lengths (9). Cross-linking between I340C and S877C also exists (10). In our model, these residue pairs are closer than 23 Å (SI Fig. 6A). In another study, R347 (TM5) is found to form a salt bridge with D924 (TM8) (11), which in the model face each other directly and their C α atoms are separated by 9 Å (SI Fig. 6A). Likewise, Therien *et al.* (12) found that TM3 and TM4 form antiparallel helices and that Q207 (TM3) and V232 (TM4) form a hydrogen bond between them, suggesting that this pair of residues are structurally close. In the model, Q207 and V232 side chains directly face each other (SI Fig. 6A).

Aside from the experimental constraints described in the main text that are satisfied by the structural model, the organization of the membrane-spanning helices also agrees with studies identifying water-accessible residues along the channel pore (13, 14). Akabas *et al.* (13) found that residues G91, K95, and Q98, which are located in TM1, are accessible to water-soluble MTS reagents, which implies that these residues line the CFTR pore. SI Fig. 6B shows that indeed these residues face the pore lining in the current model. Another study by the same group (14) found that residues I331, L333, R334, K335, F337, S341, R347, T351, R352, and Q353 (all positioned in TM6) are on the water-accessible surface of the protein. These residues in TM6 are shown to face the CFTR pore lining, which makes them accessible to water (SI Fig. 6B).

To identify the ensemble of conformations dynamically accessible to the R domain, we performed *ab initio* folding of the domain and generated decoys of low-energy structures by using discrete molecular dynamics, a rapid sampling algorithm, with an all-atom force field called Medusa (8). We clustered the decoy set to determine putatively dominant conformations of the R domain. The centroid of the largest decoy set is docked to the CFTR homology model by using ZDOCK (<http://zlab.bu.edu/libproxy.lib.unc.edu/zdock/>) (15), a rigid-body docking protocol that employs shape complementarity, desolvation energy, and electrostatics. In docking the R domain model, we imposed the constraint that the C terminus of the R domain is close to the N terminus of MSD2.

The coordinates of the CFTR model can be downloaded from <http://dokhlab.unc.edu/libproxy.lib.unc.edu/research/CFTR/>.

Construction and Expression of Mutants. cDNA coding Cys-less CFTR was produced in the pcDNA3 cloning vector by using the Stratagene QuikChange protocol as described (16). To promote maturation of the Cys-less construct, C590 and C592 were replaced with leucine, and C524 with valine. This Cys-less CFTR has a folding efficiency less than the wild type, but the molecules that mature have a single-channel conductance not different from the wild type, providing evidence of their native character. All of the constructs with cysteine mutations were introduced in this Cys-less construct. For stable expression, constructs were cotransfected with pNUT plasmid into BHK-21 cells, which were selected and maintained in methotrexate-containing medium (17). Transient expression was performed in HEK293 cells using Effectene reagent (Qiagen) according to the manufacturer's protocol. For cotransfection, the concentration of each reagent including DNA was kept the same. Cells were harvested after 40–48 h of the transfection.

Isolation of Membrane Vesicles. Membrane vesicles were isolated from BHK or HEK293 cells expressing variants of CFTR as described previously (18). To promote maturation of Cys-less CFTR variants in transiently transfected cells, dishes at 80% confluence were grown at 27°C for 48 h. The cells were harvested, pelleted, and resuspended in ice-cold hypotonic lysis buffer [10 mM Hepes (pH 7.2), 1 mM

EDTA, 2 µg/ml leupeptin, 4 µg/ml aprotinin, 250 µg/ml benzamidine, 100 µg/ml Pefabloc, 7 µg/ml E64]. After incubation on ice for 15 min, cells were lysed by 10 strokes in a Dounce homogenizer, and an equal volume of sucrose buffer [500 mM sucrose, 10 mM Hepes (pH 7.2)] was added followed by a further 15 strokes. To pellet microsomes, the postmitochondrial supernatant (10,000 'g, 10 min) was centrifuged at 100,000 'g for 45 min. The sedimented microsomes were resuspended in a buffer [250 mM sucrose, 10 mM Hepes, 5 mM MgCl₂ (pH 7.2)] to yield a total protein concentration of 1-3 mg/ml. Vesicles with a uniform diameter of ~1 µm were obtained after sonication (3 ' 20 s) and stored at -80°C until used.

Phosphorylation of CFTR. To phosphorylate CFTR, cells were incubated for 5 min in PBS supplemented with 10 µM forskolin, 100 µM DiBu-cAMP, and 1 mM 3-isobutyl-1-methylxanthine. This stimulation mixture was also present during the cross-linking reaction. To phosphorylate CFTR in membrane vesicles, membranes were treated with 100 units/ml PKA (Promega) in the presence of 2 mM ATP for 15 min at room temperature.

Cross-Linking. Cross-linking of Cys pairs in cells was performed essentially as described by Chen *et al.* (9). Briefly, CFTR-expressing cells grown on 60-mm tissue culture dishes were harvested, washed twice in PBS, and resuspended in 100 µl of PBS. Ten microliters of cell suspension was mixed with 20 µl of PBS or PBS containing 300 µM cross-linkers to yield a final concentration of 200 µM. Bifunctional cross-linkers from Toronto Research Chemicals were used: M1M (1,1-methanediyl bismethanethiosulfonate), M3M (1,3-propanediyl bismethanethiosulfonate), M8M (1,5-pentanediylyl bismethanethiosulfonate), and M17M (3,6,9,12,15-pentaoxaheptadecane-1,17-diyl bismethanethiosulfonate). To cross-link CFTR in vesicles, membranes (10 µg of total protein) were incubated with 10 µM copper phenanthroline or 10 µM M1M for 15 min. Cross-linking was reversed by reduction with 30 mM DTT. The cross-linking reaction was stopped with Laemmli sample buffer with or without DTT. Ten microliters of the samples was loaded for SDS/PAGE, and anti-CFTR mAb596 was used for Western blotting. CFTR was detected with secondary antibodies labeled with infrared dyes by using the Odyssey infrared scanner (Licor, Inc.).

CL4 Binding to NBD1. To test the binding of cytoplasmic loop 4 peptide (CL4, 1054-HLVTSLKGLWTLRAFGRQ-1071) and its disease-causing mutants (L1065P, R1066C and G1069R) to NBD1, 10 nmol of biotinylated peptides (synthesized by Abgent) was incubated with 50 µl of NeutrAvidin beads (Pierce) at room temperature for 10 min. Beads were washed four times with binding buffer to remove unbound peptides. Fifteen picomoles of purified human NBD1 was added to NeutrAvidin beads with bound peptides and incubated for 10 min at room temperature in the presence of 0.2% BSA. After extensive washing, bound proteins were eluted with SDS/PAGE sample buffer at 65°C for 5 min. Eluted samples were loaded onto 12% SDS/polyacrylamide gels for Western blot detection of NBD1 with CFTR antibody 660.

In a second assay, biotinylated CL4 or its mutant peptides L1065P and G1069R were immobilized on a Streptavidin sensor chip from BIACore. Peptides were diluted to 1 ng/µl in HBS-P buffer containing 10 mM Hepes (pH 7.4), 400 mM NaCl, 0.005% surfactant P20, and injected at 1 µl/min to reach 200 resonance units. Purified human NBD1 diluted to 1 µM in HBS-P buffer was injected at 10 µl/min for 6 min. The interaction between peptide and NBD1 was monitored by surface plasmon resonance with the BIACore 2000 instrument. To correct for nonspecific interactions, the binding of NBD1 to a control chip without peptide was subtracted from NBD1 binding to peptides.

Single-Channel Measurements. Single-channel experiments were performed as described in ref. 18. Phosphorylated microsomal membrane vesicles expressing Cys-less CFTR or other variants were fused to the preformed lipid bilayer spontaneously. A planar lipid bilayer of 1-palmitoyl-2-oleoyl-sn-glycero-3-phospho-ethanolamine and 1-palmitoyl-2-oleoyl-sn-glycero-3-phosphoserine (Avanti Polar Lipids) at a 2:1 ratio was painted over a 0.2-mm aperture in a Teflon partition between *cis* and *trans* compartments of a chamber. All measurements were done at 30°C in symmetrical salt solution containing 300 mM Tris-HCl (pH 7.2), 3 mM MgCl₂, and 1 mM EGTA. To maintain uniform channel orientation and optimal functional state, 2

mM Na₂ATP, 100 units/ml PKA, and 10 µl of membrane vesicles were added to the *cis* compartment only. Single-channel currents were measured at -75 mV under voltage-clamp conditions using an Axopatch 200B amplifier. The lower current level on all of the single-channel records shown corresponds to the open state, and the upper level corresponds to the closed state.

Values for rate equilibrium-free energy relationship (REFER) analysis were calculated as $\log(k_o) = \log(1/\tau_c)$, with $\log(K) = \log[P_o/(1-P_o)]$, where τ_c is the mean closed time, and P_o is the probability of the single channel to be open. For data analysis, the signal was digitized (Digidata 1200; Axon Instruments) with a sampling rate of 500 Hz and analyzed with pCLAMP 6.0 (Axon Instruments) software. The rate constants were calculated from the dwell-time histograms. The P_o was calculated from the all-points histogram as a ratio of the area under the peak for the open state to the total area under the both peaks on the fitted curve.

1. Riordan JR, *et al.* (1989) Identification of the cystic fibrosis gene: Cloning and characterization of complementary DNA. *Science* 245:1066-1072.
2. Callebaut I, Eudes R, Mornon JP, Lehn P (2004) Nucleotide-binding domains of human cystic fibrosis transmembrane conductance regulator: Detailed sequence analysis and three-dimensional modeling of the heterodimer. *Cell Mol Life Sci* 61:230-242.
3. Dawson RJP, Locher KP (2006) Structure of a bacterial multidrug ABC transporter. *Nature* 443:180-185.
4. Mense M, *et al.* (2006) *In vivo* phosphorylation of CFTR promotes formation of a nucleotide-binding domain heterodimer. *EMBO J* 25:4728-4739.
5. Tusnady GE, Dosztanyi Z, Simon I (2005) PDB_TM: Selection and membrane localization of transmembrane proteins in the Protein Data Bank. *Nucleic Acids Res* 33:D275-D278.
6. Chang XB, Hou YX, Jensen TJ, Riordan JR (1994) Mapping of cystic fibrosis transmembrane conductance regulator membrane topology by glycosylation site insertion. *J Biol Chem* 269:18572-18575.
7. Tusnady GE, Simon I (2001) The HMMTOP transmembrane topology prediction server. *Bioinformatics* 17:849-850.
8. Ding F, Dokholyan NV (2006) Emergence of protein fold families through rational design. *Plos Comput Biol* 2:725-733.
9. Chen EY, Bartlett MC, Loo TW, Clarke DM (2004) The ΔF508 mutation disrupts packing of the transmembrane segments of the cystic fibrosis transmembrane conductance regulator. *J Biol Chem* 279:39620-39627.
10. Wang Y, Loo TW, Bartlett MC, Clarke DM (2007) Correctors promote maturation of CFTR processing mutants by binding to the protein. *J Biol Chem* 282:33247-33251.
11. Cotten JF, Welsh MJ (1999) Cystic fibrosis-associated mutations at arginine 347 alter the pore architecture of CFTR: Evidence for disruption of a salt bridge. *J Biol Chem* 274:5429-5435.
12. Therien AG, Grant FEM, Deber CM (2001) Interhelical hydrogen bonds in the CFTR membrane domain. *Nat Struct Biol* 8:597-601.
13. Akabas MH, Kaufmann C, Cook TA, Archdeacon P (1994) Amino acid residues lining the chloride channel of the cystic fibrosis transmembrane conductance regulator. *J Biol Chem* 269:14865-14868.
14. Cheung M, Akabas MH (1996) Identification of cystic fibrosis transmembrane conductance regulator channel-lining residues in and flanking the M6 membrane-spanning segment. *Biophys J* 70:2688-2695.

15. Chen R, Li L, Weng Z (2003) ZDOCK: An initial-stage protein-docking algorithm. *Proteins* 52:80-87.
16. Cui L, *et al.* (2006) The role of cystic fibrosis transmembrane conductance regulator phenylalanine 508 side chain in ion channel gating. *J Physiol (Lond)* 572:347-358.
17. Chang XB, *et al.* (1993) Protein kinase A (PKA) still activates CFTR chloride channel after Mutagenesis of all 10 PKA consensus phosphorylation sites. *J Biol Chem* 268:11304-11311.
18. Aleksandrov AA, Riordan JR (1998) Regulation of CFTR ion channel gating by MgATP. *FEBS Lett* 431:97-101.

This Article

► [Abstract](#)
► [Full Text](#)

Services

► [Email this article to a colleague](#)
► [Alert me to new issues of the journal](#)
► [Request Copyright Permission](#)

Citing Articles

► [Citing Articles via CrossRef](#)

[Current Issue](#) | [Archives](#) | [Online Submission](#) | [Info for Authors](#) | [Editorial Board](#) | [About](#)
[Subscribe](#) | [Advertise](#) | [Contact](#) | [Site Map](#)

[Copyright © 2008 by the National Academy of Sciences](#)